DOI: 10.1002/ange.201301698

Membrane Proteins

Light-Induced Movement of the Transmembrane Helix B in Channelrhodopsin-2**

Thomas Sattig, Christian Rickert, Ernst Bamberg, Heinz-Jürgen Steinhoff, and Christian Bamann**

In the past decade, its versatile usage has established channelrhodopsin-2 (ChR2)[1] as the most prominent optogenetic tool.[2] The precise spatio-temporal control of the activity of a neuron by light allows noninvasive in vitro or in vivo investigations of neural circuits. The key is the heterologous expression of ChR2, a member of the type-I rhodopsins, that enters a photocycle upon light activation starting with the isomerization around the C13–C14 bond of its chromophore retinal.[3] The intermediates of the photocycle are linked to a closed and an open state of an ion pore. Cation flux during the open state depolarizes the cell membrane thereby triggering neuronal action potentials. A coupling of isomerization with structural alterations is well-known for bacteriorhodopsin[4] (bR) and sensory rhodopsin II[5] (SRII) that eventually leads to movement of the cytoplasmic part of transmembrane helices (TMHs) F and G. Conformational changes are also anticipated for ChR2 propagating from the chromophore to the putative cation pore.[3b,c] According to a homology model of ChR2[6] and the closed state structure of a chimera (C1C2) of ChR1 (TMHs A to E) and ChR2 (TMHs F and G),[7] the pore comprises residues from TMHs A, B, C, and G, including a ChR characteristic patch of glutamate residues in TMH B.

In this study, we followed the relative (re-)arrangements of TMHs B and F by EPR spectroscopy (double electron electron resonance, DEER) on spin-labeled mutants retaining wild-type (WT) character in ion conductance and photocycle kinetics. We could monitor a conformational change at TMH B upon light activation. Because of the unique channel properties of ChR2 and the major structural deviations in TMH A and B compared to other rhodopsins, the movement of TMH B might be a key element for channel opening.

A monomeric form of ChR2 is unknown and a cysteine-free mutant shows very low light-induced currents in electrophysiological experiments and insufficient expression in yeast cells. ChR2 cysteine mutant screening led to two constructs. The first mutant has six cysteines replaced and three remaining: C34SC36SC87SC179LC183LC259L (Mut3C). The second mutant has seven cysteines replaced and only two remaining: C34SC36SC87SC179LC183LC208AC259L (Mut2C) (Figure 1 A). Spin labeling of Mut3C with native cysteines C79, C128, and C208 using (1-oxyl-2,2,5,5-tetramethyl-pyrroline-3-methyl) methanethiosulfonate spin label (MTSSL) allows the study of interspin distances between TMHs B and TMHs F. Mut2C with native cysteines C79 and C128 reduces the analysis to interspin distances between two TMHs B sites, C79R1 and C79R1′, in the ChR2 dimer (R1 denotes the spin-labeled side chain). We found C128 to be inaccessible for MTSSL.

Light-induced currents recorded from oocytes expressing WT ChR2, Mut3C, and Mut2C (Figure 1 B) show typical inward rectification. All currents densities are normalized to the WT value at −60 mV (Figure 1 C). Mut3C shows a 14 % reduced amplitude. A further decrease to 25 % of the WT ChR2 value is found for Mut2C. The effect of the C208A mutation is also observed in a triple point mutation (C34SC36SC208A). Here, the C208A mutation shows a 28 or 12 % reduction compared to WT ChR2 or C34SC36S ChR2 (Figure 1 C), respectively. We cannot discriminate between a lower expression level and a functional defect in the C208A mutant. Amino acids other than alanine reduce the current densities even more. The sensitivity of position 208 is unclear as there is no obvious interaction site for the cysteine side chain in the chimera structure.[7]

The mutation of C79 to alanine (C34SC36SC79A) leads to a reduced current amplitude of about 52 % of the WT ChR2 value (Figure 1 C). As for C208, other mutations at position 79 (to Leu, Thr, or Ser) provoke strong current density reductions. Replacing C79 and C208 together (C34SC36SC79AC208A) creates a variant with very low current amplitude (< 10 %) comparable to that of the cysteine-less ChR2 mutant. C79 is located at the N-terminus of TMH B close to the intracellular loop A-B. This loop is not resolved in the C1C2 structure.[7] Hence, the flexibility of the loop together with the positional sensitivity of C79 could indicate a structurally relevant factor that is needed for the open state. This view is in line with a constriction site formed by the neighboring Y70 in the closed dark state structure.[7] Compared to WT ChR2 no significant change in the mono-

[*] T. Sattig,[+] Prof. Dr. E. Bamberg, Dr. C. Bamann
Abteilung für Biophysikalische Chemie
Max-Planck-Institut für Biophysik
Max-von-Laue Str. 3, 60438 Frankfurt a. M. (Germany)
E-mail: christian.bamann@biophys.mpg.de
C. Rickert,[+] Prof. Dr. H.-J. Steinhoff
Fachbereich Physik, Universität Osnabrück
Barbarastr. 7, 49076 Osnabrück (Germany)
E-mail: hsteinho@uni-osnabrueck.de
[+] These authors contributed equally to this work.

[**] This work was financially supported by the Max Planck Society, the Deutsche Forschungsgemeinschaft (grant numbers SFB 807 and SFB 944) and the Center of Excellence Frankfurt Macromolecular Complexes (to E.B.). We like to thank Heike Biehl for excellent technical assistance, Daria Dibrova (UOS) for initial modeling based on structural alignments and Rebecca Lam (MPI Biophysics) for critical reading of the manuscript.

Supporting information for this article is available on the WWW under http://dx.doi.org/10.1002/anie.201301698.

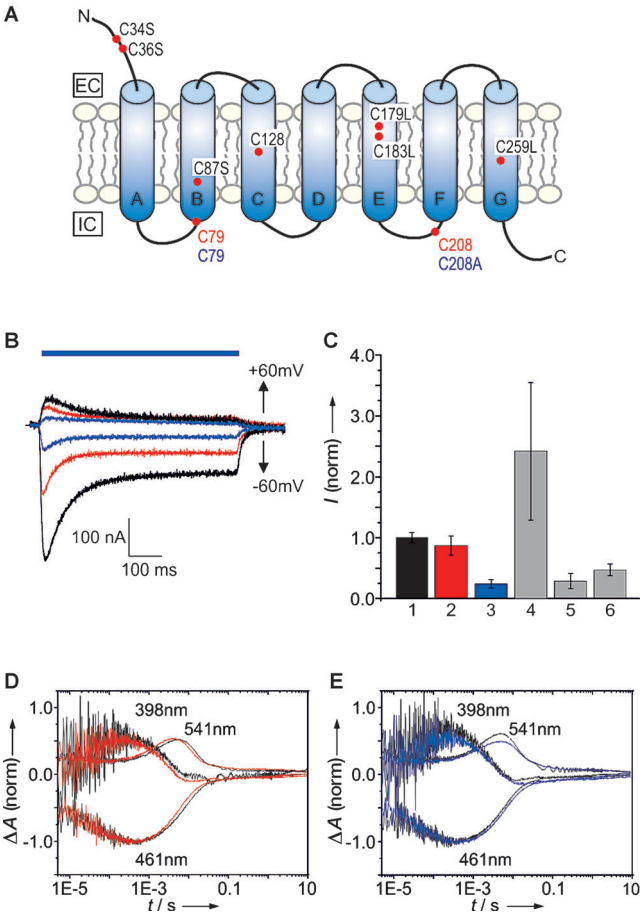

Figure 1. Characterization of ChR2 mutants. A) ChR2 and its native cysteines. The final constructs used are color coded and refer to Mut3C (red, C79 and C208) and Mut2C (blue, C79 and C208A). IC denotes the intracellular (cytoplasmic) side and EC the extracellular side. B) Light-induced currents of Mut3C (red), Mut2C (blue), and WT ChR2 (black) expressed in oocytes at two holding potentials. Illumination (380–500 nm, 4.5 $mW\,mm^{-2}$) is indicated by the blue bar. C) Current densities in pA/pF for different mutants normalized to the WT value. The bars depict the mean values ± standard error of the mean (SEM). 1 = WT ChR2 ($n = 6$), 2 = Mut3C ($n = 6$), 3 = Mut2C ($n = 6$), 4 = C34SC36S ChR2 ($n = 3$), 5 = C34SC36SC208A ChR2 ($n = 3$), 6 = C34SC36SC79A ChR2 ($n = 3$). D,E) Flash-photolysis data for Mut3C (red) and spin labeled Mut3C (black) in (D) and for Mut2C (blue) and spin labeled Mut2C (black) in (E).

valent ion selectivity is observed for Mut3C and Mut2C (see Table S1 in the Supporting Information).

Spin labeling of the purified mutants does not change the ground-state absorption spectra compared to unlabeled mutant or the WT. We followed the rise and decay of intermediate states P390, P520, and of the ground state by recording the absorption changes at 398, 541, and 461 nm for unlabeled and spin-labeled Mut2C and Mut3C (Figure 1 D, 1 E). Amplitude spectra and relaxation time constants from a global fit analysis are in accordance with the published data for WT ChR2 (Table S2).[8] As with the WT, the decay of the light-induced current coincides with the decay of the photointermediate P520 in mutants Mut3C and Mut2C. The electrophysiological and spectroscopic experiments support the conclusion that Mut3C and Mut2C show WT characteristics and the spin-labeled purified proteins do not show significantly altered kinetics.

Mut2C has two cysteines as possible targets for spin labeling: C79 and C128. According to the crystal structure C79 is solvent accessible, whereas C128 is shielded from the solvent and is found not to be accessible for MTSSL. In silico spin labeling of Mut3C based on C1C2 structure[7] using a rotamer library approach[9] reveals the C79R1—C79R1′ interspin distance distribution populated from 3.4 to 4.2 nm (Figure 2). This distance range is readily accessible by DEER spectroscopy.

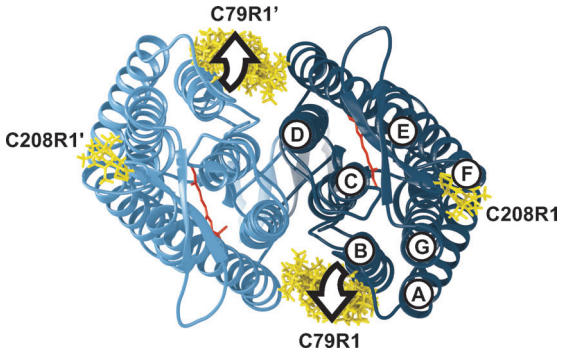

Figure 2. Structural model of a spin-labeled Mut3C dimer. View from the cytoplasmic site of the two modeled[10] protomers (light blue, dark blue) based on the C1C2 chimera (PDB code 3ug9) in ribbon diagram representation. The two corresponding retinal chromophores are depicted in orange. Spin label rotamers displayed with ball-and-stick models (yellow) cover 73 % of the total spin populations (calculated with MMM 2011).[11] The seven TMHs are labeled in one of the monomers. The putative TMH B movement as discussed in the text is indicated by the arrows.

DEER measurements were performed for the dark-adapted and the freeze-trapped illuminated states. The resulting dipolar evolution functions were background corrected and normalized (Figure 3 A). According to the modulation depth of 0.50 (0.48) the number of interacting spins of 2.3 (2.2) is in agreement with the finding of C128 not being accessible for spin labeling. The two evolution functions differ significantly from 0 to 2.0 µs. Interspin distances were determined using Tikhonov regularization as implemented in DEERAnalysis 2011.[9]

The DEER data prove a dimeric state for Mut2C even in the absence of the interprotomer disulfide bonds, which are observed in the chimera structure between the homologue residues C34 and C36.[7] The resulting distance distribution of Mut2C in the dark-adapted state (Figure 3 B, black) shows its maximum at 3.7 nm and a shoulder at 4.1 nm. The average distance agrees well with the value calculated from the crystal structure. Contrarily, the distribution for the light-induced state reveals its maximum at 4.2 nm and a shoulder at 3.8 nm. The observed structural changes are found to be fully reversible upon dark adaption. The double-peak feature is evidence for an equilibrium between two conformational states, reversibly shifting from the smaller to the larger average distance upon light activation. However, a simulated

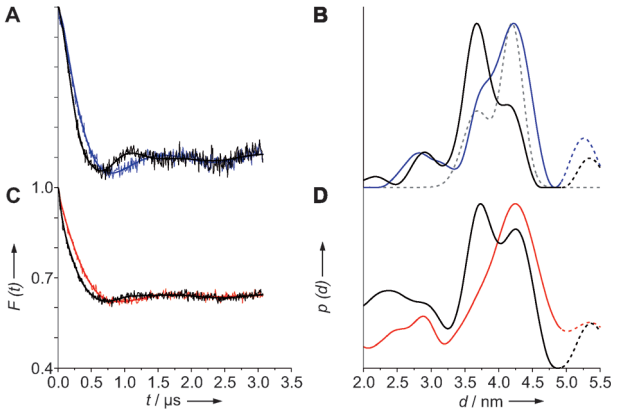

Figure 3. DEER experiments and interspin distance distributions. A) Form factor $F(t)$ of averaged DEER traces of Mut2C in the dark-adapted state (black, thin line) and upon light activation (blue, thin line). B) Fitted traces (bold lines in A) are used to calculate distance distributions for Mut2C. Distances greater than 4.8 nm are less reliable as indicated by the dotted lines. The amplitude ratio of two Gaussians fitted to the distance distribution for the dark-adapted state was inverted (gray dashed line) for comparison with the light-activated state. C) Averaged DEER traces of Mut3C in both the dark-adapted state (black, thin line) and upon light activation (red, thin line) and D) the calculated distance distributions.

occupancy inversion of two Gaussian distance populations fitted to the distribution of the dark-adapted state (Figure 3B, gray) cannot fully explain the light-induced change in the distance distribution since a further shift of the population maximum and of the descending flank of the distribution towards larger distances is observed.

In Mut3C, spin–spin interactions are expected to occur between C79R1, C79R1′, C208R1, and C208R1′ (Figure 2). The background corrected dipolar evolution functions of the dark and the illuminated states differ significantly from 0 to 1.5 µs (Figure 3C). From 3.25 to 4.5 nm the resulting distance distributions (Figure 3D) resemble those of Mut2C: the maximum at 3.7 nm in the dark state is shifted to 4.3 nm upon illumination. Compared to the distance distribution of Mut2C, additional components can be observed from 2.0 to 3.3 nm and from 4.0 to 4.8 nm, which are also altered upon illumination. Modeling including different orientations of the A–B loop reveals distances between rotamers of C79R1 and C208R1 to cover the range from 2.0 to 3.1 nm, whereas the distances between C79R1 and C208R′ are found from 3.8 to 4.7 nm, in agreement with the experimental observation. Spin labels at positions 208 and 208′ are separated by more than 4.8 nm which is beyond the distance range presently accessible. In conclusion, the DEER data of the Mut3C again show a light-induced increase of the distance between C79R1 and C79R1′. Intraprotomer (C79R1-C208R1) and interprotomer (C79R1-C208R1′) interspin distance changes were also detected.

The DEER experiments on Mut2C and Mut3C prove a light-induced increase of the average distance between C79R1 and C79R1′. A full body motion of the two protomers with respect to each other could explain this observation. However, the ChR2 dimer is exceptionally stable implying strong specific contacts between the protomers.[12] Compared to all other TMHs, B-factor analysis reveals the lowest values for TMHs C and D constituting the dimerization interface.[7] Thus, a light-induced full body motion requiring breakage of the dimerization contacts is very unlikely. More importantly, such a motion cannot explain the observed intraprotomer distance changes. We conclude that the light-induced conformational change of a ChR2 protomer implies an outward movement of C79R1 (Figure 2). This movement may be provoked by a shift and/or reorientation of TMH B (further referred to as "TMH B movement"), or a relocation of the loop connecting TMHs A and B. The crystal structure shows this loop to be already structurally disordered in the dark-adapted state, whereas the backbone of residue C79 is resolved at the N-terminus of TMH B. In agreement, the distance between C79R1 and C79R1′ is clearly defined in both the dark-adapted and light-activated states, which suggests the presence of distinct rotamer conformations indicating limited backbone flexibility. The observed distance change which may include an interchange of the rotamer populations of C79R1 is strong evidence for a movement of at least the N-terminus of TMH B.

Although small light-induced structural alterations in TMH B have been discussed for bR[13] the pronounced TMH B movement observed here is a new mode of rhodopsin conformational dynamics, which adds to the well-known displacement of TMH F observed in bR,[14] SRII,[15] and halorhodopsin.[16] A TMH B movement is in accordance with infrared data resolving large conformational differences in the protein backbone[3b,c] during the photocycle in ChR2, as known for the transition from the M1 to M2/N states in bR and SRII. The additionally observed intraprotomer (C79R1-C208R1) distance changes visible between 2.0 and 3.3 nm (Figure 3D) and the interprotomer (C79R1-C208R1′) distance changes between TMHs B and F observed between 4.5 and 4.8 nm (Figure 3D) may originate from the movement of TMH B alone or from a superposition of movements of TMHs B and F. Based on the present experiments a relocation of TMH F with respect to the other TMHs in the ChR2 protomer cannot be ruled out nor can it be proven. The helical tilt of TMH F in bR,[14b,17] allows access of water and proton transport through the hydrophobic barrier as an essential step in proton pumping.[18] In the C1C2 structure, cation permeation seems to be blocked at the cytoplasmic part of the putative pore involving TMHs A, B, C, and G. We hypothesize that the observed TMH B movement in ChR2 controls entry of water molecules and is a key element in pore opening.[6,19]

In ChR2, we expect conformational changes similar to bR, that is, a perturbation of TMH G upon retinal isomerization and its final relay to TMH F. However, in ChR2 these changes are transferred to TMH B through interaction with TMH G by a putative salt bridge between E82 and R268 and a hydrogen bond between E90 and N258. An interaction of TMH B with TMH A is possible through the hydrogen network of E97 and E101 with Q56. TMH B and TMH C are also linked by a salt bridge between E83 and H134. Sequence alignment among all twelve known ChRs reveals a strict conservation of residues E82 and E90 (both TMH B),

and R268 (TMH G).[20] While the substitution of E90 modulates the ion selectivity but leads to a functional light-gated channel,[6,21] mutation of E82 to alanine results in a severely diminished expression level of this mutant.[21b] We argue that E82 is an important structural element linking TMH B to the other TMHs, together forming the flexible cation permeation pathway. This is supported by both the observation of a strong mutation sensitivity of the C79 position and the shift in the distance distribution between the dark-adapted and the intermediate state (Figure 3B, 3D).

In summary, we demonstrate light-induced movement of TMH B. The most prominent sequence and structural differences between ChRs and other microbial-type rhodopsins are confined in TMH A and B. The investigated mutants retain their functionality as light-gated ion channels. Hence, we hypothesize that conformational changes occurring in this area are the key elements making ChR2 a cation channel.

Received: February 27, 2013
Revised: June 12, 2013
Published online: July 26, 2013

Keywords: EPR spectroscopy · ion channels · membrane proteins · optogenetics

[1] G. Nagel, T. Szellas, W. Huhn, S. Kateriya, N. Adeishvili, P. Berthold, D. Ollig, P. Hegemann, E. Bamberg, *Proc. Natl. Acad. Sci. USA* **2003**, *100*, 13940 – 13945.

[2] a) L. Fenno, O. Yizhar, K. Deisseroth, *Annu. Rev. Neurosci.* **2011**, *34*, 389 – 412; b) G. Miesenböck, *Annu. Rev. Cell. Dev. Biol.* **2011**, *27*, 731 – 758.

[3] a) C. Bamann, T. Kirsch, G. Nagel, E. Bamberg, *J. Mol. Biol.* **2008**, *375*, 686 – 694; b) E. Ritter, K. Stehfest, A. Berndt, P. Hegemann, F. J. Bartl, *J. Biol. Chem.* **2008**, *283*, 35033 – 35041; c) I. Radu, C. Bamann, M. Nack, G. Nagel, E. Bamberg, J. Heberle, *J. Am. Chem. Soc.* **2009**, *131*, 7313 – 7319.

[4] a) H. J. Steinhoff, R. Mollaaghababa, C. Altenbach, K. Hideg, M. Krebs, H. G. Khorana, W. L. Hubbell, *Science* **1994**, *266*, 105 – 107; b) H. J. Sass, G. Buldt, R. Gessenich, D. Hehn, D. Neff, R. Schlesinger, J. Berendzen, P. Ormos, *Nature* **2000**, *406*, 649 – 653; c) J. K. Lanyi, H. Luecke, *Curr. Opin. Struct. Biol.* **2001**, *11*, 415 – 419.

[5] a) J. P. Klare, E. Bordignon, M. Engelhard, H. J. Steinhoff, *Photochem. Photobiol. Sci.* **2004**, *3*, 543 – 547; b) J. L. Spudich, *Mol. Microbiol.* **1998**, *28*, 1051 – 1058.

[6] K. Eisenhauer, J. Kuhne, E. Ritter, A. Berndt, S. Wolf, E. Freier, F. Bartl, P. Hegemann, K. Gerwert, *J. Biol. Chem.* **2012**, *287*, 6904 – 6911.

[7] H. E. Kato, F. Zhang, O. Yizhar, C. Ramakrishnan, T. Nishizawa, K. Hirata, J. Ito, Y. Aita, T. Tsukazaki, S. Hayashi, P. Hegemann, A. D. Maturana, R. Ishitani, K. Deisseroth, O. Nureki, *Nature* **2012**, *482*, 369 – 374.

[8] M. K. Verhoefen, C. Bamann, R. Blöcher, U. Förster, E. Bamberg, J. Wachtveitl, *ChemPhysChem* **2010**, *11*, 3113 – 3122.

[9] G. Jeschke, V. Chechik, P. Ionita, A. Godt, H. Zimmermann, J. Banham, C. R. Timmel, D. Hilger, H. Jung, *Appl. Magn. Reson.* **2006**, *30*, 473 – 498.

[10] A. Šali, T. L. Blundell, *J. Mol. Biol.* **1993**, *234*, 779 – 815.

[11] a) Y. Polyhach, E. Bordignon, G. Jeschke, *Phys. Chem. Chem. Phys.* **2011**, *13*, 2356 – 2366; b) Y. Polyhach, G. Jeschke, *Spectrosc. Int. J.* **2010**, *24*, 651 – 659.

[12] a) M. Müller, C. Bamann, E. Bamberg, W. Kühlbrandt, *J. Mol. Biol.* **2011**, *414*, 86 – 95; b) J. Hoffmann, L. Aslimovska, C. Bamann, C. Glaubitz, E. Bamberg, B. Brutschy, *Phys. Chem. Chem. Phys.* **2010**, *12*, 3480 – 3485.

[13] N. A. Dencher, H. J. Sass, G. Büldt, *Biochim. Biophys. Acta Bioenerg.* **2000**, *1460*, 192 – 203.

[14] a) T. Hirai, S. Subramaniam, *PLoS One* **2009**, *4*, e5769; b) N. Radzwill, K. Gerwert, H.-J. Steinhoff, *Biophys. J.* **2001**, *80*, 2856 – 2866.

[15] a) A.-A. Wegener, J. P. Klare, M. Engelhard, H.-J. Steinhoff, *EMBO J.* **2001**, *20*, 5312 – 5319; b) J. P. Klare, V. I. Gordeliy, J. Labahn, G. Büldt, H.-J. Steinhoff, M. Engelhard, *FEBS Lett.* **2004**, *564*, 219 – 224; c) H. Luecke, B. Schobert, J. K. Lanyi, E. N. Spudich, J. L. Spudich, *Science* **2001**, *293*, 1499 – 1503.

[16] T. Nakanishi, S. Kanada, M. Murakami, K. Ihara, T. Kouyama, *Biophys. J.* **2013**, *104*, 377 – 385.

[17] S. Subramaniam, R. Henderson, *Nature* **2000**, *406*, 653 – 657.

[18] E. Freier, S. Wolf, K. Gerwert, *Proc. Natl. Acad. Sci. USA* **2011**, *108*, 11435 – 11439.

[19] V. A. Lórenz-Fonfría, T. Resler, N. Krause, M. Nack, M. Gossing, G. Fischer von Mollard, C. Bamann, E. Bamberg, R. Schlesinger, J. Heberle, *Proc. Natl. Acad. Sci. USA* **2013**, *110*, E1273 – E1281.

[20] a) S.-Y. Hou, E. G. Govorunova, M. Ntefidou, C. E. Lane, E. N. Spudich, O. A. Sineshchekov, J. L. Spudich, *Photochem. Photobiol.* **2012**, *88*, 119 – 128; b) F. Zhang, J. Vierock, O. Yizhar, L. E. Fenno, S. Tsunoda, A. Kianianmomeni, M. Prigge, A. Berndt, J. Cushman, J. Polle, J. Magnuson, P. Hegemann, K. Deisseroth, *Cell* **2011**, *147*, 1446 – 1457.

[21] a) K. Ruffert, B. Himmel, D. Lall, C. Bamann, E. Bamberg, H. Betz, V. Eulenburg, *Biochem. Biophys. Res. Commun.* **2011**, *410*, 737 – 743; b) Y. Sugiyama, H. Wang, T. Hikima, M. Sato, J. Kuroda, T. Takahashi, T. Ishizuka, H. Yawo, *Photochem. Photobiol. Sci.* **2009**, *8*, 328 – 336.

